Development 127, 343-354 (2000)
Printed in Great Britain © The Company of Biologists Limited 2000
DEV2495



# Essential role of Bmp7 (*snailhouse*) and its prodomain in dorsoventral patterning of the zebrafish embryo

**Alexander Dick[1,*], Marc Hild[1,*], Hermann Bauer[1,*], Yoshiyuki Imai[2], Heike Maifeld[1], Alexander F. Schier[3], William S. Talbot[2], Tewis Bouwmeester[4] and Matthias Hammerschmidt[1,‡]**

[1]Hans-Spemann Laboratory, Max-Planck Institute of Immunobiology, Stuebeweg 51, D-79108 Freiburg, Germany
[2]Department of Developmental Biology, Stanford University School of Medicine, Beckman Center B300, 279 Campus Drive, Stanford, CA 94305-5329, USA
[3]Developmental Genetics Program, Skirball Institute of Biomolecular Medicine, New York University Medical Center, New York, NY 10016, USA
[4]Developmental Biology Programme, European Molecular Biology Laboratory (EMBL), Meyerhofstrasse 1, D-69117 Heidelberg, Germany
*These authors contributed equally to the work
‡Author for correspondence (e-mail: hammerschmid@immunbio.mpg.de)

*Accepted 29 October; published on WWW 20 December 1999*

## SUMMARY

**Bone morphogenetic proteins (Bmps) are signaling molecules that have been implicated in a variety of inductive processes. We report here that zebrafish Bmp7 is disrupted in *snailhouse* (*snh*) mutants. The allele *snh$^{st1}$* is a translocation deleting the *bmp7* gene, while *snh$^{ty68}$* displays a Val→Gly exhange in a conserved motif of the Bmp7 prodomain. The *snh$^{ty68}$* mutation is temperature-sensitive, leading to severalfold reduced activity of mutant Bmp7 at 28°C and non-detectable activity at 33°C. This prodomain lesion affects secretion and/or stability of secreted mature Bmp7 after processing has occurred. Both *snh$^{st1}$* and *snh$^{ty68}$* mutant zebrafish embryos are strongly dorsalized, indicating that *bmp7* is required for the specification of ventral cell fates during early dorsoventral patterning. At higher temperature, the phenotype of *snh$^{ty68}$* mutant embryos is identical to that caused by the amorphic *bmp2b* mutation *swirl swr$^{ta72}$* and similar to that caused by the *smad5* mutation *somitabun sbn$^{dtc24}$*. mRNA injection studies and double mutant analyses indicate that Bmp2b and Bmp7 closely cooperate and that Bmp2b/Bmp7 signaling is transduced by Smad5 and antagonized by Chordino.**

Key words: Bmp7, Bmp2b, Prodomain, Dorsoventral patterning, *snailhouse*, *swirl*, Zebrafish

## INTRODUCTION

Members of the family of Bone morphogenetic proteins (Bmps) are involved in the regulation of a variety of processes during vertebrate development (reviewed in Hogan, 1996). Bmps are generated as precursors that are secreted after dimerization and proteolytic processing (Hogan, 1996). Homodimers and heterodimers of different Bmps are formed. Studies with Bmp hybrids consisting of the prodomain of one and the mature region of another Bmp protein suggest that the prodomain can influence the final activity of the mature protein by regulating the efficiency and rate of the various maturation steps and its final stability (Dale et al., 1993; Thomsen and Melton, 1993, Constam and Robertson, 1999). In target cells, Bmp signaling is transmitted by a complex of type I and type II serine-threonine transmembrane receptors. Upon ligand binding, the receptors phosphorylate and activate members of the Smad family, Smad1, Smad5 and/or Smad8, which form complexes with Smad4 and translocate to the nucleus where they participate in transcriptional complexes to regulate target gene expression (reviewed by Kretschmar and Massagué, 1998).

The biological functions of Bmps have been investigated in different species, tissues and processes (reviewed in Hogan, 1996). In *Xenopus laevis* embryos, analysis has focused on the roles of Bmp2, Bmp4 and Bmp7 during dorsoventral (DV) patterning of both the ectoderm and the mesoderm. Overexpression of *bmp2*, *bmp4* or *bmp7* and of the Bmp signaling transducers *smad1* and *smad5* (Graff et al., 1996; Suzuki et al., 1997a) leads to ventralized phenotypes, while disruption of Bmp signaling by the expression of cleavage-resistant, dominant negative ligands (Hawley et al., 1995; Suzuki et al., 1997b) or truncated, dominant negative type I receptors (Graff et al., 1994; Suzuki et al., 1994) causes dorsalization, characterized by an enlargement of dorsal mesoderm at the expense of ventral mesoderm, and an enlargment of neural tissues at the expense of epidermis. In dorsal regions, Bmp action is attenuated by secreted proteins like Follistatin, Noggin and Chordin emanating from the Spemann organizer, which bind and inactivate Bmp4 (Piccolo

et al., 1996; Zimmerman and Harland, 1996). The function of Chordin, on the contrary, is attenuated by the metalloprotease Bmp1/Tolloid, which cleaves Chordin protein, thereby promoting Bmp action (Piccolo et al., 1997; Blader et al., 1997).

Genetic data that support and extend the findings in *Xenopus* have been obtained in the zebrafish, *Danio rerio*. Large-scale mutant screens have uncovered a collection of mutants with specific defects in DV patterning (Hammerschmidt et al., 1996a; Mullins et al., 1996). Subsequent identification of the molecular nature of the mutations has revealed that the strong dorsalization of *swirl* and *somitabun* mutants is caused by mutations in the zebrafish *bmp2b* and *smad5* genes, respectively (Kishimoto et al., 1997; Nguyen et al., 1998; Hild et al., 1999), while the ventralized phenotype of *dino* mutants is due to a null mutation in zebrafish *chordin*, designated *chordino* (Schulte-Merker et al., 1997), and the weak dorsalization of *minifin* mutants due to mutations in the Chordino inhibitor Tolloid (Connors et al., 1999). Here, we investigate the role of Bmp7 during DV patterning of the zebrafish. In contrast to mouse (Dudley et al., 1995; Luo et al., 1995), *bmp7* mutant embryos display a phenotype very similar to those caused by mutations in *bmp2b* and *smad5*. Bmp7 appears to be particularly required during early phases of zebrafish DV patterning when it acts in close cooperation with Bmp2b. In addition, results obtained for the mutant allele *snh*$^{ty68}$ point to a crucial role of the Bmp7 prodomain to confer proper secretion and/or stability to mature Bmp7 protein.

## MATERIALS AND METHODS

### Cloning of zebrafish *bmp7*

A subtractive cDNA library, enriched in ventral-specific gene products, was generated by preparing a pool of cDNAs from *swirl*/*bmp2b* mutant embryos at the tailbud stage, and subtracting it from a pool of cDNAs derived from their wild-type siblings, using the Clontech PCR Select kit according to manufactor's instructions. One of the clones isolated from this library, carrying a 590 bp insert, was used as a probe to screen a gastrula cDNA library at high stringency. The contig assembled from three independent clones revealed strong homology to vertebrate *bmp7* genes. 5′ RACE was used to clone additional 262 bp not covered by the *bmp7* contig. RT-PCR with total RNA isolated with Trizol LS reagent (Gibco/BRL) from wild-type or *snh*$^{ty68}$ mutant embryos was used to clone full-length *bmp7* cDNAs in one piece; the primers used were CCGAATTCACCATGAC-TCTAAARATGTTTCCAG (sense) and CCTCTAGATTAGTGGCA-TCCGCAGGCTC (antisense). Resulting fragments were cloned using a TA cloning kit (Invitrogen).

### Mapping of *bmp7* and *bmp7-snailhouse* (*snh*$^{ty68}$) linkage analysis

*bmp7* was mapped on a panel comprising 48 individual progeny of a Tü × TL female (Gates et al., 1999), using the *bmp7* SSCP described below. Direct linkage analysis was carried out with the $F_2$ offspring of a *snh*$^{ty68}$/Tue × WIK (Rauch et al., 1997) cross, using a *bmp7* SSCP (single-strand conformational polymorphism) identified between the $P_0$ parents of the linkage cross. SSC analysis was essentially carried out as previously described (Kishimoto et al., 1997), using the following PCR conditions and primers for amplification of a *bmp7* fragment from genomic DNA of single embryos: 4 minutes 94°C – 30× (30 seconds 94°C, 1 minute 59°C, 30 seconds 72°C) – 2 minutes 72°C; sense primer, GAGCCTGCGGATGCCACTAATC; antisense primer, AAACTTGGCTCTCTGTGCAG.

### Identification and analysis of *snh*$^{st1}$

The *snh*$^{st1}$ allele was identified in a genetic screen for *N*-ethyl-*N*-nitrosourea (ENU)-induced mutations that disrupt patterning during embryogenesis (Y. I., A. F. S. and W. S. T., unpublished). In the haploid progeny of the original $F_1$ female carrying the *snh*$^{st1}$ mutation, 6% (13/217) of the embryos displayed a C5 dorsalized phenotype (Mullins et al., 1996). After recovery of *snh*$^{st1}$/+ $F_2$ individuals, additional analysis showed that *snh*$^{st1}$ fails to complement *snh*$^{ty68}$ and is transmitted in non-Mendelian ratios: crosses between *snh*$^{st1}$/+ and *snh*$^{ty68}$/+ adults gave 4.8% (84/1738) dorsalized progeny (expected 25%). The *snh*$^{st1}$ mutation was mapped using standard methods (Talbot and Schier, 1999) to analyze simple sequence length polymorphism (SSLP) markers (Knapik et al., 1998) in wild-type and *snh*$^{st1}$ mutant haploid siblings.

### Genotyping of *swr*$^{ta72}$, *sbn*$^{dtc24}$, *din*$^{tt250}$, *snh*$^{ty68}$ and *snh*$^{st1}$

Genotyping of embryos and adult fish for the *bmp2b* mutation *swr*$^{ta72}$ and the *smad5* mutation *sbn*$^{dtc24}$ was as previously described (Hild et al., 1999). The genotyping of the *chordino* allele *din*$^{tt250}$, which contains a G→A exchange in the splice donor site of the intron (TGAGCCGgtgattgt → TGAGCCGatgattgt; capital letters exon, small letters intron), downstream of the 104 bp exon deleted in *din*$^{tt250}$ cDNA (Schulte-Merker et al., 1997), and the genotyping of the *snailhouse* alleles *snh*$^{ty68}$ and *snh*$^{st1}$, is described in the ZFIN database (http://zfish.uoregon.edu/ZFIN/), 'SEARCH mutants' application, under the corresponding allele names (tt250; ty68; st1).

### Generation of constructs

For the transcription constructs, pCS2-*bmp7* and pCS2-*bmp7(snh)*, the coding region of wild-type and *snh*$^{ty68}$ *bmp7* was cloned into pCS2+ (Rupp et al., 1994) after introducing an upstream Kozak sequence (ACC) via PCR. The *snh*$^{ty68}$ mutation was introduced into pXβm-*Xbmp7* (Hawley et al., 1995) by PCR-based site-specific mutagenesis, essentially as described in Hild et al. (1999). N-terminally flag-tagged wild-type and *snh* mutant *Xbmp7* were generated as described in Hawley et al. (1995) and cloned into pCS2+ via *Eco*RI and *Xho*I restriction sites introduced by PCR. For C-terminally flag-tagged versions, wild-type and *snh Xbmp7* were PCR-amplified and cloned via *Eco*RI into pCS2flagC (A. D., unpublished).

### RNA synthesis, injection of zebrafish and *Xenopus* embryos, and *Xenopus* explant assays

For synthesis of capped mRNA with the Ambion message machine kit, pXβm-based constructs (*Xbmp7*) were linearized with *Xho*I, pSP64TS-based constructs (*bmp2b*, *smad5*) with *Sma*I, and pCS2-based constructs (*bmp7*, *smad1*, *hsmad4*) with *Not*I. For *Xenopus* animal cap experiments, synthetic RNAs were injected into both blastomeres at the 2-cell stage. At stage 9, animal caps were explanted and cultured until sibling embryos reached the indicated stage. For activin treatment, caps were cultured in 0.5× MMR; 0.5% BSA with 200 U/ml activin A. Intact caps were harvested and processed for RT-PCR analysis as previously described (Bouwmeester et al., 1996). For dorsal marginal zone (DMZ) analysis, synthetic RNAs were injected marginally into both dorsal blastomeres at the 4-cell stage. DMZs were cut at stage 9-10 and cultured until sibling embryos reached the indicated stage. Primer sequences were deduced from the Internet *XMMR* homepage.

### *Xenopus* oocyte experiments and western blots

Stage VI oocytes were manually defolliculated and injected with 10-20 ng of mRNA, encoding N-terminally and C-terminally tagged versions of Bmp7 or the point mutant Bmp7(*snh*$^{ty68}$). After 1 day incubation in 0.3× MBS, 0.1% BSA, conditioned medium (CM) and whole oocytes (WO) were harvested. WO lysates were prepared by homogenization in RIPA buffer (10 μl/oocyte) and removal of lipids by centrifugation. Equal amounts of CM and WO fractions were applied to 12.5% SDS-PAA gel electrophoresis (one WO equivalent

per lane). Western blotting was performed using standard procedures. Tagged proteins were detected with anti-FLAG M2 (IBI Kodak) monoclonal antibody at a dilution of 1:1000 and visualized with the ECL Plus detection kit (Amersham).

### Gynogenetic techniques, cell transplantation and in situ hybridization

Analyses of the *snh*$^{st1}$ mutant were carried out with haploid or homozygous diploid *snh*$^{st1}$ embryos, which were generated from heterozygous females by early pressure treatment essentially as described in Westerfield (1994). Cell transplantation experiments were carried out as described in Westerfield (1994). Whole-mount in situ hybridization with digoxigenin-labeled RNA probes was according to Hammerschmidt et al. (1996a). For *bmp7* probe synthesis, plasmid pBSK-*bmp7/2.1* was linearized with *Not*I and transcribed with T7 RNA polymerase.

## RESULTS

### Cloning of zebrafish *bmp7*

A 590 bp region of zebrafish *bmp7* was initially isolated from a wild type-*swirl* substractive library as a clone giving strongly reduced signals in in situ hybridized *swirl* mutant embryos (Fig. 1A). The complete *bmp7* coding region was subsequently cloned as described in Materials and Methods (GenBank accession number AF201379). Alignment of the deduced amino acid sequence of unprocessed zebrafish Bmp7 precursor protein with Bmp7 of *Xenopus*, mouse and human revealed moderate similarity in the prodomains and high similarity in the regions of the mature protein (Fig. 1B).

### Expression pattern of zebrafish *bmp7*

The expression pattern of zebrafish *bmp7* was investigated via developmental northern and RT-PCR analysis (Fig. 1C and not shown) and whole-mount in situ hybridization (Fig. 2). In contrast to *Xbmp7* in *Xenopus* (Nishimatsu et al., 1992; Hawley et al., 1995), zebrafish *bmp7* is not maternally expressed. Zygotic *bmp7* message was detectable from midblastula stages onwards (sphere stage), similar to *bmp2b*. In contrast, zygotic expression of *bmp4* is initiated slightly later (30% epiboly stage; Fig. 1C).

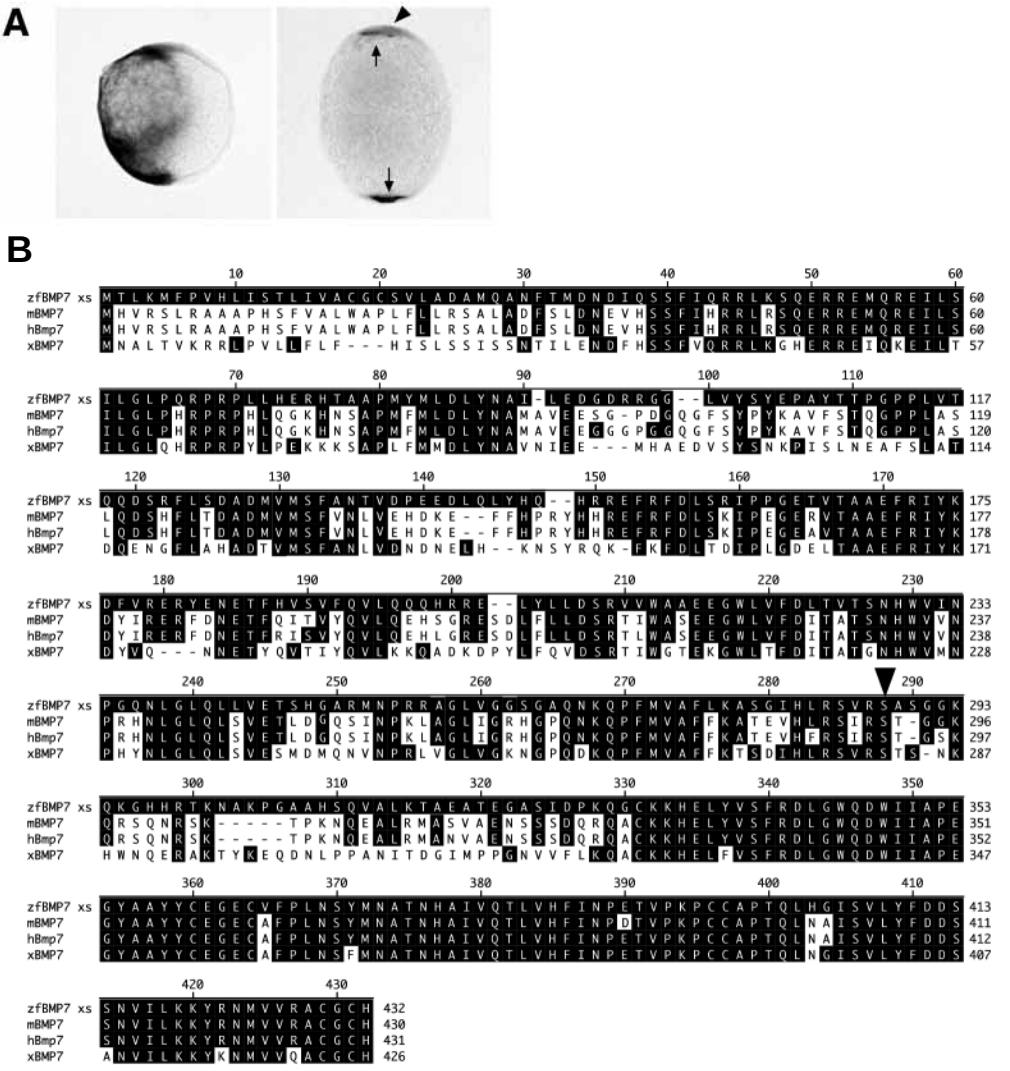


**Fig. 1.** (A) *bmp7* expression in wild-type and *bmp2b*-mutant *swr*$^{ta72}$ embryos. *swr* mutant lacks ventral *bmp7* expression, while expression in the anterior dorsal domain (arrowhead) and the yolk syncytial layer (arrows) is present. (B) Deduced amino acid sequence of zebrafish Bmp7 precursor protein aligned to Bmp7 of mouse, human and *Xenopus*. Conserved amino acid residues in black, start of mature region indicated by arrowhead. Amino acid identities of mature zebrafish Bmp7 are 79.1% to mouse and human Bmp7, 70.1% to *Xenopus* Bmp7, 69.7% to mouse Bmp5, 68.9% to mouse Bmp6, 47.5% to zebrafish Bmp2b and 51.8% to zebrafish Bmp4. (C) Temporal expression pattern of zebrafish *bmp7*, determined by developmental northern analysis, in comparison to *bmp2b*, *bmp2a* and *bmp4* (Martínez-Barberá et al., 1997). Loading control (ctr) shows ethidium-bromide-stained large rRNA.

At the sphere stage, *bmp7* is expressed broadly in the entire blastoderm with the exception of the dorsalmost regions where the fish equivalent of Spemann's organizer will form (Fig. 2A). This pattern of early *bmp7* expression appears identical to that of *bmp2b* (Nikaido et al., 1997; Hild et al., 1999). At shield stage, shortly after the onset of gastrulation, *bmp7* expression is graded, with high levels detected ventrally and progressively lower levels seen laterally and dorsally (Fig. 2B), similar to the pattern of *bmp2b* and *bmp4* (Fig. 2C,D). At this stage, *bmp7* is also expressed in cells of the fish organizer at the dorsal side of the embryo (Fig. 2B), similar to the dorsal expression of *bmp4* (Fig. 2D). In addition, *bmp7* is expressed in the yolk syncytial layer (YSL; Fig. 2B). In contrast to the ventral region, anterior-dorsal and YSL expression is not affected in the various dorsalized and ventralized mutants (Fig. 1A and data not shown).

At midgastrula stages (Fig. 2E,F) and at the end of gastrulation (Fig. 2G,J), *bmp7* is expressed in ventral marginal and ventral animal regions (presumptive ventral mesoderm and non-neural ectoderm, respectively) in a pattern very similar to that of *bmp2b* (Fig. 2H), but different from the expression pattern of *bmp4* whose transcripts are restricted to marginal regions (Fig. 2I). In DV pattern mutants (*swr*$^{ta72}$, *snh*$^{ty68}$, *sbn*$^{dtc24}$, *din*$^{tt250}$), the ventral *bmp7* expression is altered as previously reported for other ventral marker genes such as *bmp2b* (Nguyen et al., 1998; Hild et al., 1999). At the sphere stage, *bmp7* expression appears normal in all investigated mutants. However, during late blastula and gastrula stages, *bmp7* transcripts are progressively lost in the dorsalized *swr*, *snh* and *sbn* mutants, whereas the expression domain is dorsally expanded in the ventralized *din* mutant (Fig. 1A and data not shown).

At the 15-somite stage, *bmp7* displays strong expression throughout the epithelium lining the yolk sac (Fig. 2K). In addition, it is expressed in cells of the presumptive pineal gland (Fig. 2K), in the posterior neuroectoderm (Fig. 2K) and the developing endoderm (Fig. 2L). Expression in the pineal gland persists during further development (Fig. 2M,N). In addition, *bmp7* expression is maintained in ventralmost cells of the head region (Fig. 2M), and is initiated in a few epithelial cells in ventral posterior regions of the otic vesicles (Fig. 2M,O).

### *bmp7* is mutated in the dorsalized mutant *snailhouse snh*$^{ty68}$

By scoring a single-strand conformational polymorphism (SSCP) in a panel of haploid siblings (Gates et al., 1999), zebrafish *bmp7* was mapped to LG 11, between the markers z13395 and z13411 (Fig. 3A). As a first step to investigate whether the phenotype of any of the thus far unresolved dorsalized zebrafish mutants (*snailhouse*, *piggy tail*, *lost-a-fin*) might be due to a mutation in *bmp7*, direct linkage analysis between these mutations and the *bmp7* gene was performed. The *bmp7* gene was linked to *snailhouse*, and we found no recombination between *snh*$^{ty68}$ and *bmp7* in 247 mutant $F_2$ offspring (Fig. 3C).

Sequencing of *bmp7* cDNA from *snh*$^{ty68}$ mutant embryos revealed a GTG→GGG mutation leading to a Val→Gly exchange at amino acid position 130 in the proregion of Bmp7 protein (indicated in Fig. 3D). This $Val_{130}$ is conserved or replaced by an Ile in all currently known Bmp proteins, including the *Drosophila* proteins Dpp, Screw and 60A (Fig. 3D).

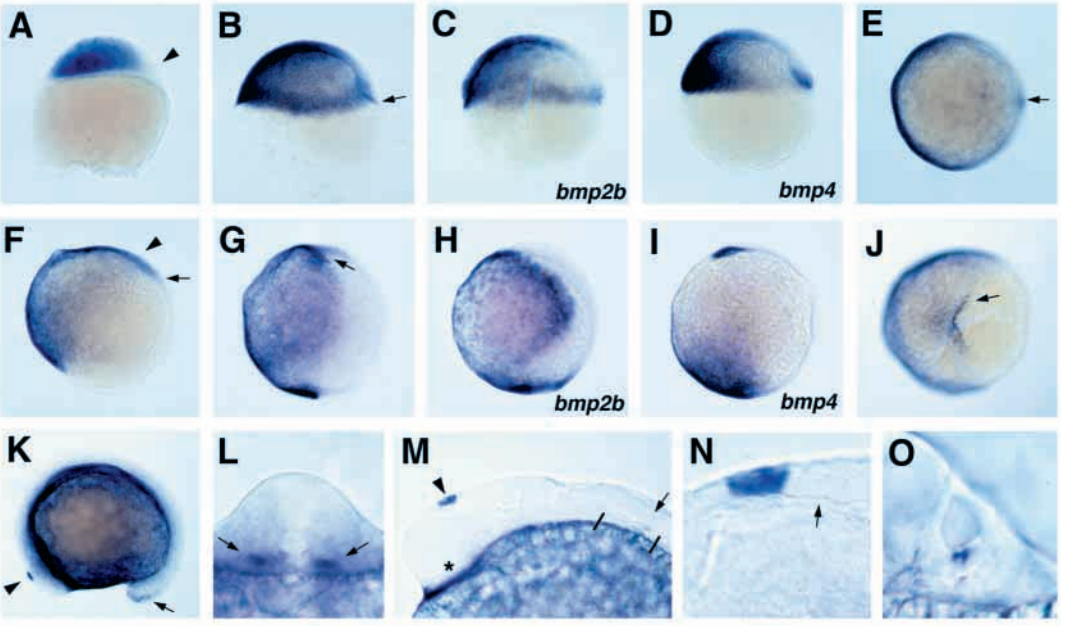


**Fig. 2.** Spatial expression pattern of *bmp7*, in comparison to *bmp2b* and *bmp4*. Unless stated otherwise, panels show *bmp7* staining. (A) *bmp7*, sphere stage, lateral view, dorsal right; dorsal side indicated by arrowhead (identified in co-stainings for *chordino* mRNA, not shown). (B-D) Shield stage, lateral view, dorsal right; (B) *bmp7*, arrow to staining in the dorsal yolk syncytial layer underlying the shield; (C) *bmp2b*; (D) *bmp4*. (E,F) *bmp7*, 80% epiboly stage, (E) animal pole up, dorsal right, optical cross section through plane indicated in F by arrow; (F) lateral view, dorsal right; arrowhead in F to anterior regions of the anterior-dorsal expression domain, arrows in E and F to posterior regions. (G-I) Tailbud-stage, lateral view, dorsal right; (G) *bmp7*, arrow to anterior-dorsal expression domain; (H) *bmp2b*; (I) *bmp4*. (J) *bmp7*, tailbud stage, animal view, dorsal right; arrow to the anterior-dorsal expression domain. (K,L) *bmp7*, 15 somite-stage; (K) lateral view, anterior left, arrowhead to presumptive pineal gland, arrow to the posterior neural tube; (L) optical cross section through trunk, arrows to two bilateral ventral stripes, most likely the endoderm. (M-O) *bmp7*, 24 hpf; (M) lateral view on head; star indicates strong expression in ventralmost cells of head region; arrowhead to expression in pineal gland; arrow to expression in a few posterior-ventral epithelial cells of the otic vesicle (indicated by bars); (N) magnified view of expression in pineal gland; arrow to ventral border of the tectum; (O) optical cross section through posterior region of otic vesicle.

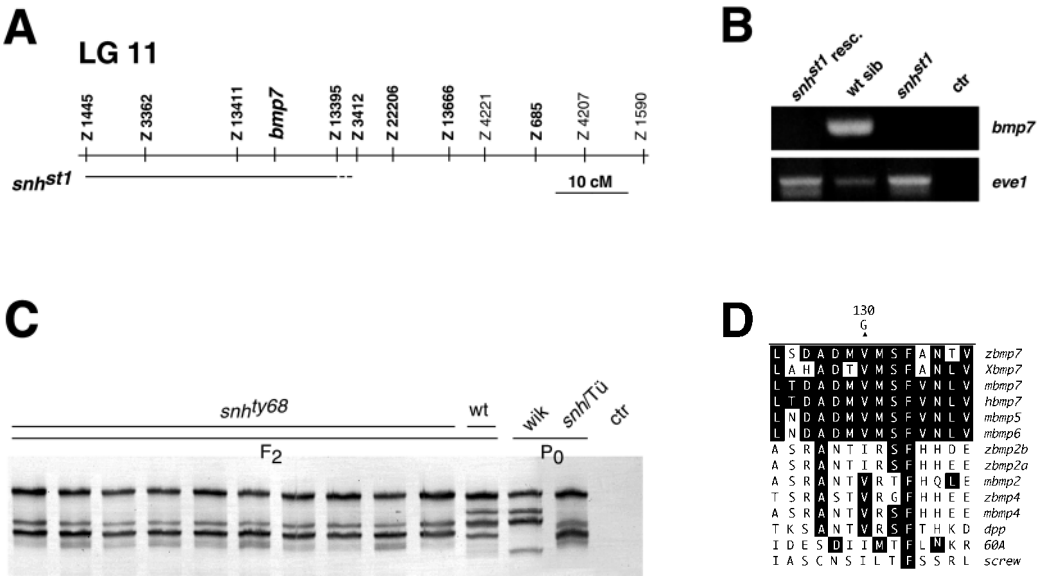


**Fig. 3.** (A) Genomic position of *bmp7* and the deletion in *snailhouse snh*$^{st1}$. SSLP markers (Knapik et al., 1998) tested on DNA of haploid *snh*$^{st1}$ mutant embryos are in bold. Z1445, Z3362, Z13411 and Z13395 gave no amplification product with mutant DNA, while Z3412, Z22206, Z13666 and Z685 did. (B) Amplification of a genomic fragment of *bmp7* and, as control, of *eve1* (Joly et al., 1993; LG 3) from *snh*$^{st1}$mutant embryos and wild-type siblings; lane 1, rescued embryo shown in Fig. 4F, at 36 hpf; lane 2, wild-type sibling at 5-somite stage; lane 3, *snh*$^{st1}$ mutant at 5-somite stage; lane 4, water control. (C) Direct linkage analysis of the *snailhouse* mutation *snh*$^{ty68}$ and *bmp7* via single strand conformational (SSC) analysis; $P_0$, parental *snh* carrier and wik wild-type fish of the linkage cross; $F_2$, single embryos of $F_2$ generation of linkage cross, *snh*$^{ty68}$, *snailhouse* mutant embryos showing C4 dorsalization, wt, sibling embryo with wild-type morphology, in this case a heterozygote; ctr, water PCR-control. (D) Alignment of the prodomain region containing the Val→Gly exchange found at amino acid position 130 of *snh*$^{ty68}$ Bmp7; amino acid residues conserved between Bmp7, Bmp5 and Bmp6 in black.

### *snh*$^{ty68}$ can be rescued by exogenous *bmp7* and has no maternal effect

As previously shown for *Xenopus bmp7* (Nguyen et al., 1998), injection of zebrafish *bmp7* mRNA can lead to a complete rescue of mutant *snh*$^{ty68}$ embryos, while the rescuing potential of other *bmps* was significantly lower (Fig. 4E; Table 2). Rescued *snh*$^{ty68}$ homozygous fish could be grown to adulthood and bred. *snh*$^{ty68}$ homozygous mutant females, when crossed to *snh*$^{ty68}$ heterozygous males, gave 50% dorsalized embryos indistinguishable from mutant offspring of two heterozygous parents (C4; Fig. 4D). When crossed to wild-type males, all offspring of *snh*$^{ty68}$ homozygous mutant females appeared wild-type (not shown). This indicates that the *snh*$^{ty68}$ mutation has no maternal effect.

### *snh*$^{ty68}$ is a temperature-sensitive hypomorph of *bmp7*

Several experiments were carried out to investigate the activity of *snh*$^{ty68}$ mutant Bmp7 protein. Assessed in injections of zebrafish embryos, *snh*$^{ty68}$ *bmp7* RNA had significantly less ventralizing activity than wild-type *bmp7*. Approximately 25-fold higher amounts of *snh*$^{ty68}$ *bmp7* RNA were necessary to achieve an effect similar to wild-type *bmp7* RNA (36% ventralized embryos with 4 pg wild-type *bmp7* RNA; 32% ventralized embryos with 100 pg *snh*$^{ty68}$ *bmp7* RNA; Table 1). A similar reduction of its ventralizing potential in zebrafish embryos was obtained for *Xenopus* Bmp7 after introduction of the corresponding Val→Gly mutation (Xbmp7$^{snh}$; Table 1). Dorsalized embryos were not obtained upon injection of *snh*$^{ty68}$ *bmp7* RNA, indicating that the *snh*$^{ty68}$ mutation, in contrast to other described mutant alleles of ventralizing agents (Kishimoto et al., 1997; Hild et al., 1999), has no antimorphic effect. In addition, we noted that the ventralizing activity of *bmp7*$^{ty68}$ is temperature sensitive: ventralizing activity of the mutant form is hardly detectable when injected embryos are incubated at 33°C (200 pg *snh*$^{ty68}$ *bmp7* RNA: 34% V2/3/4 at 28˚C, 2% V2/3/4 at 33°C; Table 1), whereas wild-type *bmp7* is fully active under these conditions (Table 1).

The activity of Xbmp7$^{snh}$ was also severely reduced

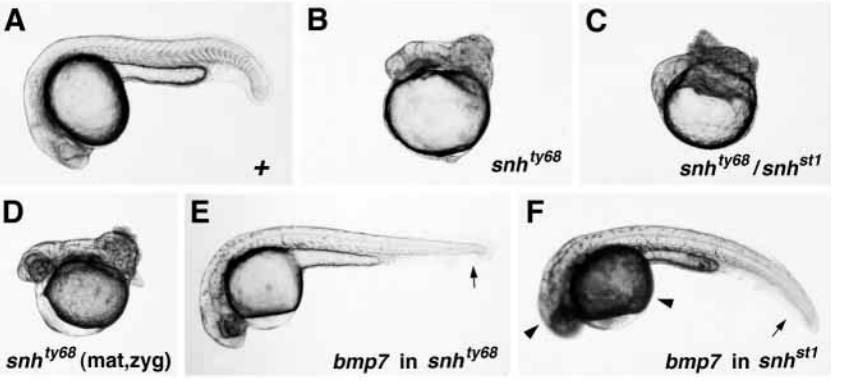


**Fig. 4.** (A-C) Non-complementation of *snh*$^{st1}$ and *snh*$^{ty68}$; 24 hpf, lateral view, anterior left; (A) wild-type sibling; (B) *snh*$^{ty68}$/ *snh*$^{ty68}$; (C) *snh*$^{ty68}$/ *snh*$^{st1}$. (D) *snh*$^{ty68}$ has no maternal effect; 36 hpf, lateral view; *snh*$^{ty68}$/ *snh*$^{ty68}$ from *snh*$^{ty68}$/ *snh*$^{ty68}$ mother, displaying C4 phenotype. (E,F) The dorsalized phenotype of *snh*$^{ty68}$ and *snh*$^{st1}$ can be rescued by injected *bmp7* mRNA; 36 hpf, lateral view; (E) rescued *snh*$^{ty68}$ embryo, with partial absence of the ventral tail fin (C1 dorsalization; arrow); (F) embryo generated by early pressure gynogenesis from *snh*$^{st1}$/+ mother, injected with *bmp7* mRNA and genotyped as *snh*$^{st1}$/*snh*$^{st1}$ (Fig. 3B); arrow to normal ventral tail fin, arrowheads to necrosing brain and brownish yolk.

**Table 1. *bmp7* RNA injections in wild-type embryos**

| RNA | pg/e | Temp. (°C) | *n* | %wt | %V1 | %V2 | %V3 | %V4 |
|---|---|---|---|---|---|---|---|---|
| *bmp7* | 2 | 28 | 118 | 95 | 5 | 0 | 0 | 0 |
| *bmp7* | 4 | 28 | 33 | 64 | 18 | 18 | 0 | 0 |
| *bmp7* | 8 | 28 | 67 | 13 | 0 | 0 | 4 | 83 |
| *bmp7* | 16 | 28 | 153 | 0 | 21 | 6 | 1 | 72 |
| *bmp7* | 100 | 28 | 149 | 0 | 0 | 0 | 0 | 100 |
| *bmp7* | 200 | 28 | 72 | 0 | 0 | 0 | 0 | 100 |
| *bmp7$^{snh}$* | 2 | 28 | 57 | 100 | 0 | 0 | 0 | 0 |
| *bmp7$^{snh}$* | 4 | 28 | 42 | 100 | 0 | 0 | 0 | 0 |
| *bmp7$^{snh}$* | 8 | 28 | 48 | 100 | 0 | 0 | 0 | 0 |
| *bmp7$^{snh}$* | 16 | 28 | 36 | 94 | 6 | 0 | 0 | 0 |
| *bmp7$^{snh}$* | 100 | 28 | 91 | 68 | 0 | 20 | 0 | 12 |
| *bmp7$^{snh}$* | 200 | 28 | 92 | 57 | 9 | 8 | 1 | 25 |
| *Xbmp7* | 2 | 28 | 23 | 100 | 0 | 0 | 0 | 0 |
| *Xbmp7* | 100 | 28 | 88 | 0 | 13 | 2 | 0 | 84 |
| *Xbmp7$^{snh}$* | 100 | 28 | 68 | 99 | 1 | 0 | 0 | 0 |
| *bmp7 Cflag* | 50 | 28 | 28 | 68 | 18 | 14 | 0 | 0 |
| *bmp7$^{snh}$Cflag* | 50 | 28 | 96 | 96 | 4 | 0 | 0 | 0 |
| *bmp7 Nflag* | 50 | 28 | 47 | 0 | 0 | 0 | 0 | 100 |
| *bmp7$^{snh}$Nflag* | 50 | 28 | 36 | 73 | 0 | 17 | 10 | 0 |
| *bmp7* | 100 | 28 | 48 | 0 | 0 | 2 | 0 | 98 |
| *bmp7* | 100 | 33 | 38 | 0 | 0 | 0 | 0 | 100 |
| *bmp7$^{snh}$* | 100 | 28 | 34 | 73 | 3 | 15 | 9 | 0 |
| *bmp7$^{snh}$* | 100 | 33 | 40 | 95 | 5 | 0 | 0 | 0 |
| *bmp7* | 200 | 28 | 72 | 0 | 0 | 0 | 0 | 100 |
| *bmp7* | 200 | 33 | 83 | 0 | 0 | 0 | 7 | 93 |
| *bmp7$^{snh}$* | 200 | 28 | 92 | 57 | 9 | 8 | 1 | 25 |
| *bmp7$^{snh}$* | 200 | 33 | 66 | 86 | 12 | 2 | 0 | 0 |

Classification of ventralization strength from weak (V1) to strong (V4) was according to Kishimoto et al. (1997). Abbreviations: pg/e, pg injected mRNA per embryo; Temp, incubation temperature of embryos; *n*, number of scored embryos; wt, wild type.

compared to wild-type Xbmp7 in several *Xenopus* explant assays. First, Xbmp7$^{snh}$ only weakly counteracted the effect of a cleavage-resistant, dominant negative version of Xbmp7, CM-Xbmp7 (Hawley et al., 1995) on neural induction (Fig. 5A). Secondly, Xbmp7$^{snh}$ was less active in its ability to interfere with dorsal mesoderm induction (Fig. 5B,C). Finally, Xbmp7$^{snh}$ displayed a strongly reduced potential to induce ventral mesoderm in animal cap explants (Fig. 5D; Nishimatsu and Thomsen, 1998).

Together, these data indicate that *snh$^{ty68}$* is a strong hypomorph of *bmp7* and that the dorsalized phenotype of *snh$^{ty68}$* mutant zebrafish embryos is caused by the observed $Val_{130}$→Gly exchange in the proregion of Bmp7.

## The *snh$^{ty68}$* mutation affects secretion or stability of secreted mature Bmp7 protein

Bmp proteins are synthesized as precursors that are processed and secreted after dimer formation (see for review Hogan, 1996). The amino acid exchange found in *snh$^{ty68}$* Bmp7 does not reside in the biologically active mature protein, but in the prodomain that is cleaved off during maturation. To elucidate why the *snh$^{ty68}$* mutation nevertheless leads to such a strong reduction in activity, experiments with flag-tagged versions of wild-type and mutant *Xbmp7* were carried out in *Xenopus* oocytes. RNA encoding either N-terminally (prodomain region) or C-terminally (mature region) tagged Bmp7 proteins were injected, and oocyte lysates and conditioned media were analyzed for Bmp7 precursors and processing products in western blots and immunoprecipitations. Upon injection of the RNAs into zebrafish embryos, the N-terminally flagged Bmp7 proteins showed normal ventralizing activity like the untagged versions, whereas the activity of C-terminally tagged proteins displayed strongly reduced activities, suggesting that the tag might interfere with the biological activity of mature Bmp7 (Table 1). When injected in *Xenopus* oocytes, all four RNAs (C- and N-terminally tagged wild-type and *snh* mutant *bmp7*) gave rise to similar amounts of Bmp7 precursor proteins, as revealed on Western blots of oocyte lysates (Fig. 5E, left panel). In addition, identical amounts of tagged mature Bmp7 protein were observed, indicating that *snh$^{ty68}$* mutant Bmp7 is normally processed (Fig. 5E, left panel). In contrast to the lysate, however, strongly reduced amounts of *snh* Bmp7 processing products (mature protein for C-terminally tagged version and prodomain peptide for N-terminally tagged version) were found in the conditioned medium (Fig. 5E, middle panel). This suggests that the *snh$^{ty68}$* mutation leads to a strongly impaired secretion of Bmp7 or to instability of the secreted Bmp7 processing products. Under non-reducing conditions, both wild-type and *snh* mutant precursor Bmp7 proteins ran at higher molecular weight, indicating that Bmp7 dimerization is not affected by the *snh$^{ty68}$* mutation (Fig. 5E, right panel; oocyte lysate not shown).

## *bmp7* is deleted in the dorsalized mutant *snh$^{st1}$*

In the initial large-scale zebrafish mutant screens, only one *snailhouse* allele was identified (Mullins et al., 1996). We have subsequently isolated additional dorsalized mutants. One of these mutants, designated *snh$^{st1}$*, does not complement *snh$^{ty68}$*;

crosses of *snh*$^{ty68}$ and *snh*$^{st1}$ heterozygous fish gave dorsalized embryos with a slightly stronger phenotype than *snh*$^{ty68}$ homozyous mutant embryos (Fig. 4B,C). Fragments of *bmp7* failed to amplify from genomic DNA of *snh*$^{st1}$ homozygotes (Fig. 3B), indicating that the *bmp7* gene is deleted in *snh*$^{st1}$. Testing SSLP markers located on the same linkage group as *bmp7* (Knapik et al., 1998) revealed that a >30 cM region of LG11 is deleted in *snh*$^{st1}$ mutants (Fig. 3A). Additional mapping experiments indicate that *snh*$^{st1}$ is a translocation (Y. I., A. F. S., and W. S. T., unpublished). The region absent in *snh*$^{st1}$ mutants is large and includes genes other than *bmp7*. However, rescue experiments suggest that the dorsalized phenotype of *snh*$^{st1}$ embryos results from the loss of *bmp7*: upon injection of wild-type *bmp7* mRNA into *snh*$^{st1}$ mutant embryos, the strong dorsalized phenotype could be rescued to almost wild-type condition or converted to a ventralized phenotype, depending on the amount of injected *bmp7* mRNA (Fig. 5F; Table 2). Such rescued homozygous mutant embryos develop later defects including brain necrosis. They die at around 48 hours after fertilization, most likely due to the lack of other essential genes removed by the deletion.

## The phenotype of *snailhouse* mutant embryos

*snailhouse snh*$^{ty68}$ mutant embryos have been previously reported to display a dorsalization slightly weaker (C4) than that of the *bmp2b* mutant *swr*$^{ta72}$ (C5; Mullins et al., 1996; Nguyen et al., 1998). The expression pattern of *krox20* (Oxtoby and Jowett, 1993), for instance, reveals an expansion of hindbrain rhomobomeres 3 and 5 into ventralmost regions of *swirl*/*bmp2b* mutant *swr*$^{ta72}$ embryos (Fig. 6C; Nguyen et al., 1998) while, in *snailhouse snh*$^{ty68}$, these rhombomeres are only partially expanded (Fig. 6B; Nguyen et al., 1998). A phenotype indistinguishable from that of *swr*$^{ta72}$ mutants, however, was obtained for *snh*$^{ty68}$ mutant embryos, when they were incubated at higher temperature (33°C; Fig. 6D). Wild-type sibling embryos incubated at 33°C developed normally. At 21°C, the *snh*$^{ty68}$ phenotype was slightly weaker than at 28°C (C3 instead of C4, Mullins et al., 1996; not shown). This temperature sensitivity of the phenotypic strength of *snh*$^{ty68}$ mutant embryos is consistent with the aforementioned temperature-sensitive effect of *snh*$^{ty68}$ *bmp7* RNA in overexpression studies. The dorsalized phenotype of *snh*$^{st1}$ mutant embryos is at least as strong as that of *swr*$^{ta72}$ and *snh*$^{ty68}$ at 33°C, with a complete expansion of both *krox20* expression domains (Fig. 6E; Table 2). However, compared to the other mutants, the *krox20* stripes appear shifted anteriorly, suggesting that the head region of *snh*$^{st1}$ mutants is compressed (see Discussion). Together, the data suggest that at 33°C, the *snh*$^{ty68}$ mutation can be regarded as a *bmp7* null, and that the phenotype caused by the loss of *bmp7* is as strong as that caused by the loss of Bmp2b activity in *swirl* mutants.

## *snh*$^{ty68}$ acts non-cell autonomously

It has been recently reported that *bmp2b*, when misexpressed in single cells in ectopic locations, acts cell autonomously to induce epidermal specification during ectoderm patterning of the zebrafish embryo (Nikaido et al., 1999), suggesting that *bmp2b* action is restricted to cells in which it is expressed.

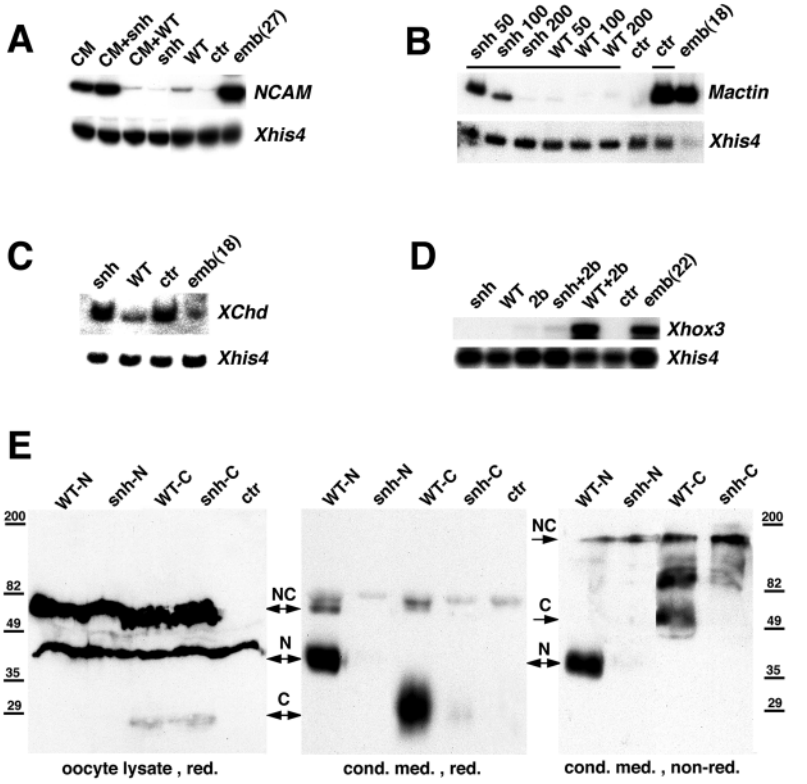


**Fig. 5.** (A-D) RT-PCR analyses of RNA-injected *Xenopus* explants to compare the activity of wild-type (WT) and *snh*$^{ty68}$ mutant Xbmp7(snh). The stage of control embryos (emb) is indicated in brackets; ctr, uninjected control explants. (A) *N-CAM* and, as control, *Xhis* mRNA levels, in animal cap explants. Wild-type, but not *snh*$^{ty68}$ mutant *Xbmp7* RNA attenuates the neural-inducing properties of a cleavage-resistant, dominant negative version of Xbmp7 (CM) in co-injected caps (CM+WT, CM+snh). (B) *Mactin* and *Xhis* mRNA levels in animal cap explants treated with the mesoderm-inducer activin (indicated with bar). Injection of 50 pg of wild-type *Xbmp7* RNA per embryo (WT 50) is sufficient to repress activin-induced transcription of the dorsal mesodermal marker gene muscle *actin*, while 200 pg *snh* mutant RNA (snh 200) are required to achieve the same effect. (C) *XChd* (Sasai et al., 1994) and *Xhis4* mRNA levels in dorsal marginal zone explants. Injected wild-type, but not *snh* mutant *Xbmp7* RNA leads to decreased mRNA levels of the dorsal mesodermal marker gene *chordin*. (D) *Xhox3* and *Xhis3* mRNA levels of animal cap explants. Coinjected wild-type *Xbmp7* and *bmp2b* RNA (WT+2b) induce high-level expression of the ventral mesodermal marker gene *Xhox3*, while co-injected *snh* mutant *Xbmp7* and *bmp2b* RNA (snh+2b) and the three different RNAs alone do not (snh, WT, 2b). (E) Western blot analysis with anti-flag antibodies of lysates and conditioned media (cond. med.) from *Xenopus* oocytes injected with RNA encoding N- or C-terminally tagged wild-type (WT-N, WT-C) or *snh*$^{ty68}$ mutant (snh-N, snh-C) zebrafish Bmp7. ctr, un-injected control oocytes; red., reducing SDS-PAGE conditions; non-red., non-reducing conditions. Tagged precursor protein is marked with NC, cleaved proregion peptide with N and mature protein with C. In the left panel, N could not be addressed, due to a contaminant band of the oocyte lysate. Similar amounts of wild-type and *snh* NC and C are found in the oocyte lysates, whereas in the conditioned medium, levels of snh-C and snh-N are strongly reduced compared to WT-C and WT-N. Under non-reducing conditons (right panel), NC and C shift to higher molecular weights, while N does not.

**Table 2. RNA injections in mutant embryos**

| RNA | pg/e | Cross | Temp (°C) | *n* | %C5 | %C4 | %C3 | %C2 | %C1 | %wt | %V1 | %V2 | %V3 | %V4 | % resp mut |
|---|---|---|---|---|---|---|---|---|---|---|---|---|---|---|---|
| *bmp2b* | 0.25 | *snh*$^{+/-}$f × *snh*$^{+/-}$m | 28 | 148 | 0 | 2 | 2 | 18 | 1 | 77 | 0 | 0 | 0 | 0 | 76 |
| *bmp2b* | 0.25 | *snh*$^{+/-}$f × *snh*$^{-/-}$m | 33 | 97 | 20 | 15 | 6 | 9 | 2 | 47 | 0 | 1 | 0 | 0 | 30 |
| *bmp2b* | 1 | *snh*$^{+/-}$f × *snh*$^{+/-}$m | 28 | 45 | 0 | 0 | 0 | 0 | 0 | 0 | 27 | 8 | 28 | 37 | 100 |
| *bmp2b* | 2 | *snh*$^{+/-}$f × *snh*$^{+/-}$m | 28 | 60 | 0 | 0 | 0 | 0 | 0 | 0 | 0 | 0 | 24 | 76 | 100 |
| *bmp2b* | 0.25 | *swr*$^{+/-}$f × *swr*$^{+/-}$m | 28 | 174 | 4 | 1 | 1 | 3 | 15 | 66 | 3 | 3 | 4 | 0 | 80 |
| *bmp2b* | 1 | *swr*$^{+/-}$f × *swr*$^{+/-}$m | 28 | 46 | 0 | 0 | 0 | 0 | 2 | 0 | 35 | 11 | 17 | 35 | 100 |
| *bmp2b* | 2 | *swr*$^{+/-}$f × *swr*$^{+/-}$m | 28 | 57 | 0 | 0 | 0 | 0 | 0 | 23 | 5 | 2 | 15 | 55 | 100 |
| - | - | *sbn*$^{+/-}$f × *sbn*$^{+/-}$m | 28 | 70 | 0 | 26 | 74 | 0 | 0 | 0 | 0 | 0 | 0 | 0 | |
| *bmp2b* | 1 | *sbn*$^{+/-}$f × *sbn*$^{+/-}$m | 28 | 54 | 0 | 0 | 0 | 0 | 23 | 20 | 6 | 31 | 20 | 0 | 100 |
| *bmp7* | 2 | *snh*$^{+/-}$f × *snh*$^{+/-}$m | 28 | 335 | 0 | 0 | 0 | 0 | 21 | 76 | 0 | 3 | 0 | 0 | 100 |
| *bmp7* | 4 | *snh*$^{+/-}$f × *snh*$^{+/-}$m | 28 | 106 | 0 | 0 | 0 | 0 | 7 | 43 | 8 | 0 | 41 | 8 | 100 |
| *bmp7* | 2 | *swr*$^{+/-}$f × *swr*$^{+/-}$m | 28 | 192 | 5 | 13 | 2 | 0 | 4 | 75 | 0 | 1 | 0 | 0 | 28 |
| *bmp7* | 4 | *swr*$^{+/-}$f × *swr*$^{+/-}$m | 28 | 80 | 0 | 14 | 0 | 6 | 10 | 43 | 15 | 6 | 4 | 2 | 44 |
| *bmp7* | 16 | *swr*$^{+/-}$f × *swr*$^{+/-}$m | 28 | 39 | 0 | 0 | 0 | 0 | 0 | 3 | 6 | 6 | 0 | 85 | 100 |
| – | – | *sbn*$^{+/-}$f × *sbn*$^{+/-}$m | 28 | 35 | 0 | 75 | 25 | 0 | 0 | 0 | 0 | 0 | 0 | 0 | |
| *bmp7* | 2 | *sbn*$^{+/-}$f × *sbn*$^{+/-}$m | 28 | 18 | 0 | 67 | 33 | 0 | 0 | 0 | 0 | 0 | 0 | 0 | 0 |
| *bmp7* | 4 | *sbn*$^{+/-}$f × *sbn*$^{+/-}$m | 28 | 52 | 0 | 23 | 46 | 19 | 12 | 0 | 0 | 0 | 0 | 0 | 12 |
| *bmp7* | 16 | *sbn*$^{+/-}$f × *sbn*$^{+/-}$m | 28 | 237 | 0 | 2 | 2 | 2 | 0 | 0 | 0 | 0 | 0 | 94([b]) | 96 |
| – | – | *snh*$^{st1\ +/-}$f EP ([a]) | 28 | 86 | 11 | 0 | 0 | 0 | 0 | 89 | 0 | 0 | 0 | 0 | |
| *bmp7* | 2 | *snh*$^{st1\ +/-}$f EP ([a]) | 28 | 62 | 3 | 0 | 0 | 0 | 0 | 97 | 0 | 0 | 0 | 0 | 69 |
| *bmp7* | 50 | *snh*$^{st1\ +/-}$f EP ([a]) | 28 | 45 | 0 | 0 | 0 | 0 | 0 | 4 | 0 | 0 | 2 | 94 | 100 |
| *smad1* | 50 | *snh*$^{-/-}$f × *snh*$^{+/-}$m | 28 | 39 | 0 | 18 | 0 | 13 | 8 | 5 | 18 | 28 | 10 | 0 | 64 |
| *smad1* | 50 | *snh*$^{-/-}$f × *snh*$^{+/-}$m | 33 | 55 | 20 | 0 | 0 | 4 | 2 | 24 | 8 | 39 | 4 | 0 | 27 |
| *smad5* | 50 | *snh*$^{+/-}$f × *snh*$^{-/-}$m | 28 | 48 | 0 | 0 | 25 | 25 | 0 | 50 | 0 | 0 | 0 | 0 | 50 |
| *smad5* | 50 | *snh*$^{+/-}$f × *snh*$^{-/-}$m | 33 | 54 | 39 | 0 | 2 | 3 | 2 | 54 | 0 | 0 | 0 | 0 | 22 |
| *smad5* | 100 | *snh*$^{+/-}$f × *snh*$^{+/-}$m | 33 | 86 | 2 | 2 | 0 | 4 | 0 | 39 | 12 | 12 | 19 | 2 | 84 |
| *hsmad4* | 100 | *snh*$^{-/-}$f × *snh*$^{-/-}$m | 28 | 25 | 0 | 100 | 0 | 0 | 0 | 0 | 0 | 0 | 0 | 0 | 0 |

Used alleles, unless stated otherwise, were *snailhouse snh*$^{ty68}$, *swirl swr*$^{ta72}$ and *somitabun sbn*$^{dtc24}$. Classification of dorsalization (strong C5-weak C1) and ventralization (weak V1-strong V4) strength was according to Mullins et al. (1996) and Kishimoto et al. (1997).

% resp mut, frequency of mutant embryos showing a response to the injected RNA. Response was defined as a shift of the mutant phenotype to an at least two classes weaker phenotypic strength, e.g. C5 to at least C3 for *swr* or *snh* at 33°C, C4 to at least C2 for *snh* at 28°C or *sbn*. Response frequencies were calculated relative to the expected frequencies of mutant embryos in the various crosses.

([a]) embryos were generated by early pressure treatment of haploid offspring of a heterozygous *snh*$^{st1}$ female. The low frequency of obtained mutant embryos in the control (11% instead of 50%) is due to non-Mendelian segregation of the mutation and the distance between deletion and centromere. Injected embryos were scored as C5 by their typical elongated shape at the tailbud stage and lysis around the 15-somite stage (Mullins et al., 1996). Surviving injected embryos were subjected to genotyping at 36 hours after fertilization.

([b]) V4 phenotypes obtained after injection of *bmp7* mRNA into *sbn* mutant embryos appear slightly different from the regular V4 phenotype described in Kishimoto et al (1997) and obtained in all other injections. Like regular V4 embryos, they lack head and notochord and form large, blocky somites. However, all structures develop at the former animal pole of the embryo, and no tail grows out.

Abbreviations: f, female; m, male; see also Table 1. *hsmad4*, RNA encoding human Smad4, as described in Hild et al. (1999), which in contrast to *sbn* mutants (Hild et al. 1999) was ineffective in *snh*.

Here, we investigated the behavior of Bmp7 during ectoderm patterning in *snh* wild-type chimeras. Labeled cells of sphere stage *snh*$^{ty68}$ mutant embryos deriving from a cross of two *snh*$^{ty68}$ homozygous parents were transplanted into wild-type (WT) recipients of the same stage, and chimeric embryos were scored after 24 hours of development for the presence of labeled cells in the ventral tail fin, a tissue completely absent in *snh*$^{ty68}$ mutant embryos. We found labeled *snh* mutant cells in the ventral tail fins of 14.5% (16/110) of the examined *snh* →WT chimeric embryos, in comparison to 20.5% (8/39) in chimeras from WT→WT control transplantations (Fig. 7). Similar ratios were found for other tissues, such as the central nervous system, which contained labeled cells in 81% (89/110) of the *snh* →WT chimeras, and in 90% (35/39) of the WT→WT chimeras. This indicates that Bmp7 acts non-cell autonomously during ectoderm patterning of the zebrafish embryo, inducing epidermal specification in neighboring *bmp7* mutant cells.

### Genetic interaction of *snh*/*bmp7* with *swr*/*bmp2*, *sbn*/*smad5* and *chordino*

Several experiments were carried out to examine the interaction of Bmp7 with other known players of DV pattern formation. In the case of *bmp2b*, *smad5* and *chordino*, for which zebrafish mutants have been identified (Kishimoto et al., 1997; Nguyen et al., 1998; Hild et al., 1999; Schulte-Merker et al., 1997), double mutants with the *bmp7* allele *snh*$^{ty68}$ were analyzed. The *bmp2b* allele *swr*$^{ta72}$ and the antimorphic *smad5* allele *sbn*$^{dtc24}$ both have a weak dominant zygotic effect, leading to weakly dorsalized phenotypes of heterozygous embryos (up to C1), characterized by partial loss of the ventral tailfin (Fig. 8A,C; Mullins et al., 1996). The phenotype of *swr*/*snh* and *sbn*/*snh*

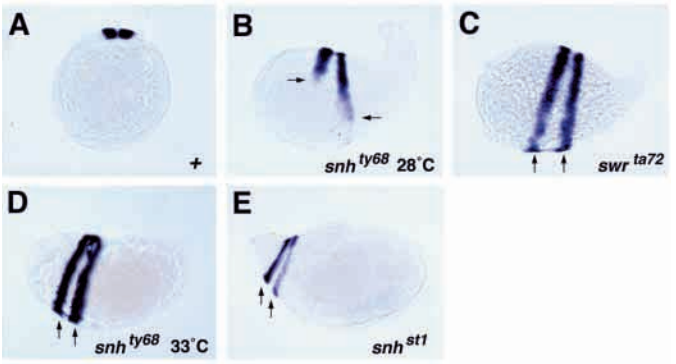


**Fig. 6.** *krox20* expression in *snailhouse* and *swirl* mutants, 5-somite stage, lateral view, anterior left. (A) Wild-type sibling; rhombomeres 3 and 5 are indicated; (B) $snh^{ty68}$/ $snh^{ty68}$ at 28°C; (C) $swr^{ta72}$/ $swr^{ta72}$; (D) $snh^{ty68}$/ $snh^{ty68}$ at 33°C; (E) $snh^{st1}$/ $snh^{st1}$. Horizontal arrows point to the ventral border of the *krox20* stripes; vertical arrows indicate that stripes are fused on the ventral side of the embryo.

double heterozygotes kept at 33°C was significantly stronger, up to C4 dorsalization, characterized by completely coiled tails and trunks (Fig. 8A-D; $swr^{ta72}$/+ m × $snh^{ty68}$/+ f: 78% wild type, 22% C2-C4; *n*=121; in this background, $swr^{ta72}$ itself had no visible dominant effect; $sbn^{dtc24}$/+ m × $snh^{ty68}$/+ f: 48% wild type, 30% C1; 22% C4; *n*=72).

At 28°C, *swr*, *snh* double heterozygotes developed much weaker phenotypes and could be raised to adulthood. Intercrosses of *swr*, *snh* double heterozygotes yielded 45% C5 embryos at 33°C, which in contrast to C4 embryos display a rupture of the yolk sac around the 15-somite stage (Mullins et al., 1996; *n*=525, 4 crosses). Fifteen of those C5 dorsalized embryos with indistinguishable phenotypes were genotyped after photography at the 5-somite stage (not shown). 2/15 were *snh*, *swr* double homozygous, 7/15 homozygous for *swr* and heterozygous or wild type for *snh*, and 6/15 homozygous for *snh* and heterozygous or wild type for *swr* (expected ratio 1:3:3), indicating that the phenotype of *snh*, *swr* double mutants is not stronger than that of *snh* and *swr* single mutants (expected frequency for C5 embryos: 43.75%).


**Fig. 7.** Chimeric embryos after transplantation of labeled cells from a $snh^{ty68}$ homozygous donor mutant into a wild-type recipient (*snh*→WT) or, as control, from a wild-type donor embryo into a wild-type recipient (WT→WT); 24 hpf, lateral view on tail.

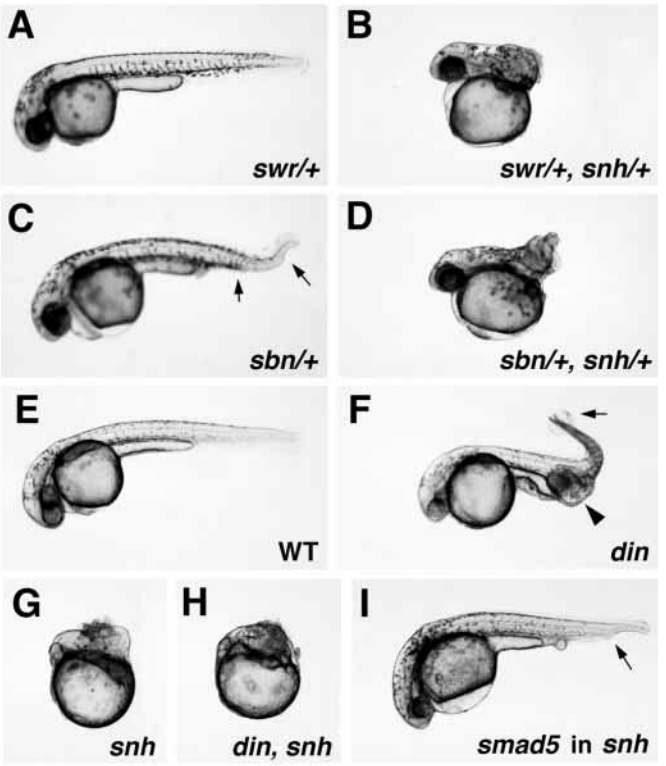


**Fig. 8.** (A-D) Genetic interaction of $snh^{ty68}$ with $swr^{ta72}$ and $sbn^{dtc24}$ in double heterozygotes from crosses of a *snh* heterozygous female with a *swr* or a *sbn* heterozygous male; 36 hpf, lateral view, anterior left. Embryos were incubated at 33°C. (A) *swr*/+ sibling, with no obvious dorsalized phenotype; (B) putative *snh*/+, *swr*/+, with C4 dorsalization (wound up tail and trunk; Mullins et al., 1996); (C) *sbn*/+, with weak C2 dorsalization (lack of ventral tail fin, kinked up tail tip; arrows; Mullins et al., 1996); (D) putative *snh*/+, *sbn*/+, with C4 dorsalization. (E-H) $snh^{ty68}$ is epistatic to *chordino* $din^{tt250}$; 32 hpf, lateral view; (E) wild-type sibling; (F) *dino* sibling, with enlarged blood islands (arrowhead) and extra ventral tail fins (arrow); (G,H) embryos with C4 dorsalization, genotyped as *snh*/*snh*, *din*/+ (G) and *snh*/*snh*, *din*/*din* (H). (I) Rescued $snh^{ty68}$ mutant embryo with C1 dorsalization (arrow to ventral tail fin) after injection of *smad5* mRNA (50 pg/embryo) and incubation at 33°C, 36 hpf.

We also investigated the phenotype of *bmp7*, *chordino* double mutant embryos from a cross of two $snh^{ty68}$, $din^{tt250}$ double heterozygous parents. Loss of Chordino function normally leads to strongly ventralized embryos (V3; Fig. 8F; Hammerschmidt et al., 1996a; Schulte-Merker et al., 1997). $snh^{ty68}$, $din^{tt250}$ double homozygotes, however, displayed a strongly dorsalized phenotype (C4) which was indistinguishable from that of $snh^{ty68}$ homozygotes (Fig. 8G,H; found (and expected) segregation pattern: 25.2% (25%) C4, 17.4% (18.75%) V3, 57.4% (56.25%) wild type; *n*=389; 4 crosses). This indicates that *bmp7* is epistatic to *chordino*, suggesting that Chordino acts as an inhibitor of Bmp7, similar to previous findings for Chordino and Bmp2b (Hammerschmidt et al., 1996b).

### *snh* mutant embryos can be rescued by exogenous *bmp2b*, *smad1* or *smad5* mRNA

To investigate the order of gene functions in the pathway of ventral specification, *bmp2b*, *bmp7*, *smad1* and *smad5*, all of

which have ventralizing activities, were overexpressed in the various dorsalized mutants (compare Nguyen et al., 1998). Amounts of injected mRNAs were varied to allow a direct comparison of their activities in the different mutants. At 28°C, *bmp2b* rescued *snh*$^{ty68}$/*bmp7* as well as its own mutant *swr*$^{ta72}$ (76-80%; Table 2) while, at 33°C, the rescue frequency of *snh* mutants was lower (30%; Table 2). Similarly, *bmp7* was more effective in its own mutant *snh*$^{ty68}$ than in the *bmp2b* mutant *swr* (Table 2). Thus, it appears that, although both exogenous *bmp2b* and *bmp7* RNA are most effective in mutants in their own genes, excessive amounts can also compensate for the loss of the other. Rescue of the *smad5* mutant *somitabun* by *bmp7*, however, was approximately 4-fold-less efficient than for *bmp2b*/*swr* mutants and 8-fold-less efficient than for *bmp7*/*snh* mutants (Table 2; 4 pg/e), while *bmp2b* rescued *bmp2b*/*swr* and *smad5*/*sbn* mutants similarly well (Table 2; 1 pg/e).

We also compared the rescuing potentials of Smad1 and Smad5, the two putative receptor-activated transducers of Bmp signaling. We have previously shown that *sbn* mutants can be rescued by both *smad1* and *smad5* (Hild et al., 1999), whereas *swr* mutants only respond to *smad1*, but not to *smad5* mRNA (Dick et al., 1999). *snh* mutants, like *sbn*, but unlike *swr*, responded equally well to exogenous *smad1* and *smad5* mRNA at both 28°C or 33°C (Table 2; Fig. 8I).

## DISCUSSION

We have identified the Bone morphogenetic factor Bmp7 as an essential protein of zebrafish DV patterning. Two alleles are described, *snailhouse snh*$^{ty68}$, which was isolated during the Tübingen large scale mutant screen (Mullins et al., 1996), and the newly isolated allele *snh*$^{st1}$. While *snh*$^{ty68}$ contains a temperature-sensitive point mutation, *snh*$^{st1}$ appears to be a translocation which removes approximately 30 cM of LG 11, including the *bmp7* gene. Our finding that the *snh*$^{st1}$ DV phenotype can be rescued by injection of *bmp7* RNA might indicate that it is solely caused by the loss of the *bmp7* gene. However, overexpression of *bmp7* also leads to a rescue of other dorsalized mutants like the *bmp2b* mutant *swr* (LG 20) and the *smad5* mutant *sbn* (LG 14). Thus we cannot rule out that the *snh*$^{st1}$ rescue is due to a combined compensation for *bmp7* and additional, thus far unidentified essential genes deleted in the *snh*$^{st1}$ chromosome. Such a loss of additional DV regulators could explain why *snh*$^{st1}$ mutant embryos display a compression of the head region compared to *snh*$^{ty68}$ mutants at 33°C and *swr*$^{ta72}$ mutants. A similar head compression was also observed for another dorsalized mutant with a stronger phenotype than that of *swr*$^{ta72}$ (unpublished observation). Therefore, all epistasis analyses were carried out with *snh*$^{ty68}$, which appears to serve as a null allele at 33°C.

### Bmp7 function in zebrafish

*snailhouse* mutant embryos are strongly dorsalized, indicating that *bmp7* is required to specify ventral cell fates during early DV patterning of the zebrafish embryo. Several observations suggest that Bmp7 fulfills this role in close cooperation with Bmp2b: both genes show very similar temporal and spatial expression patterns, null mutations in both genes (*snh*$^{ty68}$ at 33°C and *swr*$^{ta72}$) cause indistinguishable phenotypes, and both genes are epistatic to the Bmp antagonist *chordino*. Furthermore, the two mutations interact genetically with each other and with the *smad5* mutation *sbn*$^{dtc24}$, and the phenotype of *bmp2b*, *bmp7* double homozygous mutants is not stronger than that of *bmp7* or *bmp2b* single mutants. Thus, *bmp2b* and *bmp7* appear to act at similar positions of the same pathway, maybe as Bmp2b/Bmp7 heterodimers, as has been shown for Bmp2 and Bmp7 in several other instances (Sampath et al., 1990; Nishimatsu and Thomsen, 1998, and references therein). Alternatively, Bmp2b and Bmp7 could signal via parallel pathways, which converge at the level of Smad5. This, however, would mean that signaling via each of the two pathways is absolutely essential for Smad5 activation.

We also detected differences between *bmp7*/*snh* and *bmp2b*/*swr*. First, *bmp2b* mRNA could more efficiently rescue the *smad5*/*sbn* mutant phenotype than *bmp7* mRNA, consistent with previous results obtained in a comparison of *bmp2b* with *Xenopus Xbmp7* (Nguyen et al., 1998). In addition, *bmp7*/*snh* mutant embryos could be equally well rescued by *smad1* and *smad5* mRNA (this paper), while *bmp2b*/*swr* mutants only responded to *smad1* (Dick et al., 1999). For *bmp2b*/*swr*, this differential response to Smad1 and Smad5 had let us propose a model with distinct functions of Bmps and Smads during different phases of DV patterning. During an early phase, the putative morphogenetic Bmp gradient is set up, involving positive Bmp autoregulation mediated by Smad5 and Bmp inhibition by Chordino signaling from the organizer. Later, this Bmp gradient is interpreted and cell fates are specified independently of Smad5, involving Bmp signal transduction by Smad1 (Hild et al., 1999; Dick et al., 1999). According to this model, exogenously supplied Smad5 is sufficient to compensate for the loss of essential upstream Bmp signaling during the early, but not during the late phase of DV patterning. Thus, our finding that *snh*$^{ty68}$, in contrast to *swr*$^{ta72}$, can be rescued by *smad5* RNA injection suggests that *bmp7*, in contrast to *bmp2b*, is dispensable for the late phase of DV patterning. Rather, *bmp7* (together with *bmp2b*) appears to be required for the early, Smad5-dependent phase to set up the putative Bmp gradient. It remains unclear how such a shift from a *bmp7*-dependent to a more *bmp7*-independent state could be achieved. Recruitment of a new receptor with higher affinity to Bmp2b homodimers could be one mechanism. Such differences in the specifity to the various ligands has been reported for the Bmp type I receptors ALK-2, ALK-3 and ALK-6 in COS cell culture studies (ten Dijke et al., 1994).

### Bmp7 function in other vertebrates

A similar function during early ventral cell fate specification has been proposed for *Xbmp7* in *Xenopus* embryos. *Xbmp7* is expressed throughout the presumptive ectoderm and mesoderm of blastula and gastrula stage embryos. Overexpression studies and studies with a cleavage-resistant, dominant negative version (CM) indicate that *Xbmp7* is involved in ventral specification of ectoderm and mesoderm (Hawley et al., 1995; Suzuki et al., 1997b; Nishimatsu and Thomsen, 1998). However, these studies, in contrast to the zebrafish data presented here, did not allow any conclusions about the requirement of Xbmp7 during DV patterning, since CM-Xbmp7 in addition to Xbmp7 itself also inhibits proper processing of other Bmps like Xbmp4 (Hawley et al., 1995).

In early mice and chicken embryos, *bmp7* is most prominently expressed in dorsal regions, corresponding to the

expression in prechordal plate and anterior notochord in zebrafish, while ventral expression, in contrast to zebrafish and *Xenopus*, is initiated later and at much weaker levels (Lyons et al., 1995; Dale et al., 1997). During later stages of mouse development, *bmp7* is most prominently expressed in distinct regions of the neural tube, optic and otic vesciles, heart, gut, mesonephros, limb buds, and developing cartilage and bone (Lyons et al., 1995), again different from the later expression pattern of *bmp7* in zebrafish. In addition, *bmp7*-deficient mouse embryos display a rather normal early DV pattern (Dudley et al., 1995; Luo et al., 1995). Thus, *bmp7* in mouse and chicken, although acting in concert with Bmp2 and antagonized by Chordin like in fish and amphibia (Sampath et al., 1990; Lyons et al., 1995; Dale et al., 1999), is apparently not involved in early ventral specification, but in other developmental processes like midline signaling (Dale et al., 1997), nephrogenesis, skeletogenesis and eye development (Dudley et al., 1995; Luo et al., 1995).

### The Bmp7 prodomain

The mutant Bmp7 allele *snh$^{ty68}$* with its Val→Gly exchange in the prodomain also allows some insights into the importance of the prodomain for the biological activity of the mature protein. Bmp precursor proteins are supposed to be processed intracellularly, after dimer formation and before secretion (Hogan, 1996). For *snh$^{ty68}$* mutant Bmp7, normal levels of the precursor and the mature protein were found in *Xenopus* oocyte lysates, indicating that stability and processing of the precursor are not affected by the mutation. However, we found dramatically reduced amounts of both the prodomain peptide and the mature protein in the conditioned medium, which could be due either to impaired secretion or to reduced stability of the processing products after they have been secreted. The fact that intracellular levels of mutant mature protein are unaltered might argue against a defect in the secretion process itself, although additional experiments will be necessary to clarify this point. A similar effect of prodomains on the stability of secreted mature protein has been recently reported for two other TGFβ-family proteins, mouse Bmp4 and Nodal (Constam and Robertson, 1999). Our data provide genetic evidence for an essential role of the prodomain on the secretion and/or turnover of mature TGFβ polypeptides.

We thank Beate Fischer for technical help during the analysis of the *din$^{tt250}$* mutation on genomic DNA level, Andrea Meier for carrying out in situ hybridizations, Dr Trevor Jowett for *krox20* in situ probe, Dr David Grunwald for cDNA libraries, and Dr Mary Mullins for communicating data prior to publication. This work was supported by the Max-Planck Gesellschaft, fellowships from the Boehringer Ingelheim Fonds, Stuttgart (A. D.), the Yamada Science Foundation and the Uehara Memorial Foundation (Y. I.), NIH grants R01GM57825 (W. S. T.), RO1GM56211 and R21HG01704 (A. F. S.), and the Pew Scholars Program (W. S. T.). A. F. S. is a Scholar of the McKnight Endowment Fund for Neuroscience.

## REFERENCES

**Blader, P., Rastegar, S., Fischer, N. and Strähle, U.** (1997). Cleavage of the BMP-4 antagonist Chordin by zebrafish Tolloid. *Science* **278**, 1937-1940.

**Bouwmeester, T., Kim, S. H., Sasai, Y., Lu, B. and De Robertis, E. M.** (1996). Cerberus is a head-inducing secreted factor expressed in the anterior endoderm of Spemann´s organizer. *Nature* **382**, 595-601.

**Connors, S. A., Trout, J., Ekker, M. and Mullins, M. C.** (1999). The role of *tolloid*/*minifin* in dorsoventral pattern formation of the zebrafish embryo. *Development* **126**, 3119-3130.

**Constam, D. B. and Robertson, E. J.** (1999). Regulation of Bone Morphogenetic Protein activity by pro domains and proprotein convertases. *J. Cell. Biol.* **144**, 139-149.

**Dale, L., Matthews, G. and Colman, A.** (1993). Secretion and mesoderm-inducing activity of the TGF-β-related domain of Xenopus Vg1. *EMBO J.* **12**, 4471-4480.

**Dale, J. K., Vesque, C., Lints, T., Sampath, T. K., Furley, A., Dodd, J. and Placzek, M.** (1997). Cooperation of BMP7 and SHH in the induction of forebrain ventral midline cells by prechordal mesoderm. *Cell* **90**, 257-269.

**Dale, J. K., Sattar, N., Heemskerk, J., Clarke, J. D. W., Placzek, M. and Dodd, J.** (1999). Differential patterning of ventral midline by axial mesoderm is regulated by BMP7 and Chordin. *Development* **126**, 397-408.

**Dick, A., Meier, A. and Hammerschmidt, M.** (1999). Smad1 and Smad5 have distinct roles during dorsoventral patterning of the zebrafish embryo. *Dev. Dyn.* **216**, 285-298.

**Dudley, A. T., Lyons, K. M. and Robertson, E. J.** (1995). A requirement for bone morphogenetic protein-7 during development of the mammalian kidney and eye. *Genes Dev.* **9**, 2795-2807.

**Gates, M. A., Kim, L., Egan, E. S., Cardozo, T., Sirotkin, H. I., Dougan, S. T., Laskari, D., Abagyan, R., Schier, A. F. and Talbot, W. S.** (1999). A genetic linkage map for zebrafish: comparative analysis of genes and expressed sequences. *Genome Res.* **9**, 334-347.

**Graff, J. M., Thies, R. S., Song, J. J., Celeste, A. J. and Melton, D. A.** (1994). Studies with a *Xenopus* BMP receptor suggest that ventral mesoderm-inducing signals override dorsal signals in vivo. *Cell* **79**, 169-179.

**Graff, J. M., Bansal, A. and Melton, D. A.** (1996). *Xenopus* Mad proteins transduce distinct subsets of signals for the TGFβ superfamily. *Cell* **85**, 479-487.

**Hammerschmidt, M., Pelegri, F., Mullins, M. C., Kane, D. A., van Eeden, F. J. M., Granato, M., Brand, M., Furutani-Seiki, M., Haffter, P., Heisenberg, C.-P.** et al. (1996a). *dino* and *mercedes*, two genes regulating dorsal development in the zebrafish embryo. *Development* **123**, 95-102.

**Hammerschmidt, M., Serbedzija, G. N. and McMahon, A. P.** (1996b). Genetic analysis of dorsoventral pattern formation in the zebrafish: Requirement of a BMP-like ventralizing activity and its dorsal repressor. *Genes Dev.* **10**, 2452-2461.

**Hawley, S. H. B., Wünnenberg-Stapleton, K., Hashimoto, C., Laurent, M. N., Watabe, T., Blumberg, B. W. and Cho, K. W. Y.** (1995). Disruption of BMP signals in embryonic Xenopus ectoderm leads to direct neural induction. *Genes Dev.* **9**, 2923-2935.

**Hild, M., Dick, A., Rauch, J. G., Meier, A., Bouwmeester, T., Haffter, P. and Hammerschmidt, M.** (1999). The *smad5* mutation *somitabun* blocks Bmp2b signaling during early dorsoventral patterning of the zebrafish embryo. *Development* **126**, 2149-2159.

**Hogan, B. L. M.** (1996). Bone morphogenetic proteins: multifunctional regulators of vertebrate development. *Genes Dev.* **10**, 1580-1594.

**Joly, J.-S., Joly, C., Schulte-Merker, S., Boulkebache, H. and Condamine, H.** (1993). The ventral and posterior expression of the homeobox gene *eve1* is perturbed in dorsalized and mutant embryos. *Development* **119**, 1261-1275.

**Kishimoto, Y., Lee, K.-H., Zon, L., Hammerschmidt, M. and Schulte-Merker, S.** (1997). The molecular nature of *swirl*: BMP2 function is essential during early dorsoventral patterning. *Development* **124**, 4457-4466.

**Knapik, E. W., Goodman, A., Ekker, M., Chevrette, M., Delgado, J., Neuhauss, S., Shimoda, N., Driever, W., Fishman, M. C. and Jacob, H. J.** (1998). A microsatellite genetic linkage map for zebrafish (*Danio rerio*). *Nature Genet.* **18**, 338-343.

**Kretschmar, M. and Massagué, J.** (1998). SMADs: mediators and regulators of TGF-β signaling. *Curr. Opin. Gen. Dev.* **8**, 103-111.

**Luo, G., Hofman, C., Bronckers, A. L. J. J., Sohocki, M., Bradley, A. and Karsenty, G.** (1995). BMP-7 is an inducer of nephrogenesis, and is also required for eye development and and skeletal patterning. *Genes Dev.* **9**, 2808-2820.

**Lyons, K. M., Hogan, B. L. M. and Robertson, E. J.** (1995). Colocalization of BMP7 and BMP2 RNAs suggests that these factors cooperatively mediate tissue interactions during murine development. *Mech. Dev.* **50**, 71-83.

**Martínez-Barberá, J. P., Toresso, H., Da Rocha, S. and Krauss, S.** (1997). Cloning and expression of three members of the zebrafish Bmp family: *Bmp2a*, *Bmp2b* and *Bmp4*. *Gene* **198**, 53-59.

**Mullins, M. C., Hammerschmidt, M., Kane, D. A., Odenthal, J., Brand, M., Eeden van, F. J. M., Furutani-Seiki, M., Granato, M., Haffter, P., Heisenberg, C.-P.** et al. (1996). Genes establishing dorsoventral pattern formation in the zebrafish embryo: the ventral specifying genes. *Development* **123**, 81-93.

**Nguyen, V. H., Schmid, B., Trout, J., Conners, S. A., Ekker, M. and Mullins, M. C.** (1998). Ventral and lateral regions of the zebrafish gastrula, including the neural crest progenitors, are established by a *bmp2b*/*swirl* pathway of genes. *Dev. Biol.* **199**, 93-110.

**Nikaido, M., Tada, M., Saij, T. and Ueno, N.** (1997). Conservation of BMP signaling in zebrafish mesoderm patterning. *Mech. Dev.* **61**, 75-88.

**Nikaido, M., Tada, M., Takeda, H., Kuroiwa, A. and Ueno, N.** (1999). In vivo analysis using variants of zebrafish BMPR-1A: range of action and involvement of BMP in ectoderm patterning. *Development* **126**, 181-190.

**Nishimatsu, S., Suzuki, A., Shoda, A., Murakami, K. and Ueno, N.** (1992). Genes for Bone morphogenic proteins are differentially transcribed in early amphibian embryos. *Biochem. Biophys. Res. Comm.* **186**, 1487-1495.

**Nishimatsu, S.-i. and Thomsen, G. H.** (1998). Ventral mesoderm induction and patterning by bone morphogenetic protein heterodimers in *Xenopus* embryos. *Mech. Dev.* **74**, 75-88.

**Oxtoby, E. and Jowett, T.** (1993). Cloning of the zebrafish Krox-20 (Krx-20) and its expression during hindbrain development. *Nucleic Acids Res.* **21**, 1087-1095.

**Piccolo, S., Agius, E., Lu, B., Goodman, S., Dale, L. and DeRobertis, E. M.** (1997). Cleavage of Chordin by Xolloid metalloprotease suggests a role for proteolytic processing in the regulation of Spemann organizer activity. *Cell* **91**, 407-416.

**Piccolo, S., Y., Sasai, Y., Lu, B. and De Robertis, E. M.** (1996). A possible molecular mechanism for Spemann organizer function: inhibition of ventral signals by direct binding of Chordin to BMP-4. *Cell* **85**, 589-598.

**Rauch, G.-J., Granato, M. and Haffter, P.** (1997). A polymorphic zebrafish line for genetic mapping using SSLPs on high-percentage agarose gels. *Technical Tips Online* **T01208**.

**Rupp, R. A. W., Snider, L. and Weintraub, H.** (1994). *Xenopus* embryos regulate the nuclear localization of XMyoD. *Genes Dev.* **8**, 1311-1323.

**Sampath, T. K., Coughlin, J. E., Whetstone, R. M., Banach, D., Corbett, C., Ridge, R. J., Özkaynak, E., Oppermann, H. and Rueger, D. C.** (1990). Bovine osteogenic protein is composed of dimers of OP-1 and BMP-2A, two members of the transforming growth factor-β superfamily. *J. Biol. Chem.* **265**, 13198-13205.

**Sasai, Y., Lu, B., Steinbeisser, H., Geissert, D., Gont, L. K. and De Robertis, E. M.** (1994). *Xenopus chordin*: a novel dorsalizing factor activated by organizer-specific homeobox genes. *Cell* **79**, 779-790.

**Schulte-Merker, S., Lee, L. J., McMahon, A. P. and Hammerschmidt, M.** (1997). The zebrafish organizer requires *chordino*. *Nature* **387**, 862-863.

**Suzuki, A., Thies, R. S., Yamayi, N., Song, J. J., Wozney, J. M., Murakami, K. and Ueno, N.** (1994). A truncated bone morphogenetic protein receptor affects dorsal-ventral patterning in the early *Xenopus* embryo. *Proc. Natl. Acad. Sci. USA* **91**, 10255-10259.

**Suzuki, A., Chang, C., Yingling, J. M., Wang, X.-F. and Hemmati-Brivanlou, A.** (1997a). Smad5 induces ventral fates in *Xenopus* embryo. *Dev. Biol.* **184**, 402-405.

**Suzuki, A., Kaneko, E., Ueno, N. and Hemmati-Brivanlou, A.** (1997b). Regulation of epidermal induction by BMP2 and BMP7 signaling. *Dev. Biol.* **189**, 112-122.

**Talbot, W. S. and Schier, A. F.** (1999). Positional cloning of mutated zebrafish genes. *Methods Cell Biol.* **60**, 259-286.

**ten Dijke, P., Yamashita, H., Sampath, T. K., Reddi, H., Estevez, M., Riddle, D. L., Ichijo, H., Heldin, C.-H. and Miyazono, K.** (1994). Identification of type I receptors for Osteogenic Protein-1 and Bone Morphogenetic Protein-4. *J. Biol. Chem.* **269**, 16985-16988.

**Thomsen, G. H. and Melton, D. A.** (1993). Processed Vg1 protein is an axial mesoderm inducer in *Xenopus*. *Cell* **74**, 433-441.

**Westerfield, M.** (1994). *The Zebrafish Book: A Guide for the Laboratory use of Zebrafish*. University of Oregon Press.

**Zimmerman, L. B. and Harland, R. M.** (1996). Bmp-4 function is blocked by high affinity binding to the Spemann organizer signal Noggin. *Cell* **85**, 599-606.